Tough interface-enabled stretchable electronics using nonstretchable polymer semiconductors and conductors

Jiheong Kang^{1,2†}, Jaewan Mun^{1†}, Yu Zheng¹, Masato Koizumi³, Naoji Matsuhisa¹, Hung-Chin Wu¹, Shucheng Chen¹, Jeffrey B.-H. Tok¹, Gae Hwang Lee⁴, Lihua Jin³*& Zhenan Bao¹*

¹ Department of Chemical Engineering, Stanford University, Stanford, California 94305, USA.

² Department of Materials Science and Engineering, Korea Advanced Institute of Science and Technology (KAIST), Daejeon, 34141 Republic of Korea

³ Department of Mechanical and Aerospace Engineering, University of California, Los Angeles, CA 90095- 1597, USA.

⁴ Samsung Advanced Institute of Technology Yeongtong-gu, Suwon-si, Gyeonggi-do 443-803, South Korea

[†]These authors contributed equally: Jiheong Kang, Jaewan Mun

*To whom correspondence should be addressed:

E-mail: zbao@stanford.edu (Z.B.), lihuajin@seas.ucla.edu (L.J.)

Semiconducting polymer thin films are essential elements of soft electronics for both wearable and biomedical applications¹⁻¹¹. However, high-mobility semiconducting polymers are usually brittle and can be easily fractured under small strains (<10%)¹²⁻¹⁴. Recently, improved intrinsic mechanical properties of semiconducting polymer films have been reported through molecular design ¹⁵⁻¹⁸ and nanoconfinement¹⁹. Here we show that engineering the interfacial properties between a semiconducting thin film and a substrate can significantly delay micro-crack formation in the film. We present a universal design strategy that involves covalently bonding a dissipative interfacial polymer layer, consisting of dynamic non-covalent crosslinks, between a semiconducting thin film and a substrate. This enables high interfacial toughness between the layers, suppression of delamination, and delocalization of strain. As a result, crack initiation and propagation are significantly delayed to much higher strains. Specifically, the crack onset strain of a high-mobility semiconducting polymer thin film improved from 30% strain to 110 % strain without any noticeable microcracks. Despite the presence of a large mismatch in strain between the plastic semiconducting thin film and an elastic substrate after unloading, the tough interface layer helped maintain bonding and exceptional cyclic durability and robustness. Furthermore, we found that our interfacial layer reduces the mismatch of thermal expansion coefficients between different layers. This approach can improve crack onset strain of various semiconducting polymers, conducting polymers and even metal thin films.

Freestanding plastic thin films, such as polymers and metals, rupture primarily due to strain localization onto film defects²⁰. However, when such a thin film is supported on a polymer substrate, strain localization may be mitigated by the substrate, so that the thin film becomes more tolerant to elongation and deformation. For example, a thin copper film (100 nm) on a polyimide substrate could sustain > 50% strain; whereas a freestanding copper thin film breaks

below 2% strain^{21,22}. Recently, Choi and coworkers reported crack suppression in a copper thin film (100 nm) through improving the film adhesion on the substrate using electron beam irradiation²³. Furthermore, Zhao and Suo reported design strategies for tough interfaces between hydrogels and various solids^{24–27}. One main concept is to introduce energy dissipation mechanisms into hydrogels, in conjunction with forming covalent bonding between the two materials. As a result, the interfacial toughness was significantly increased^{25, 26}. However, such tough interface strategies have not been applied to stretchable polymer electronics.

Here, we present a tough interface (TI) design to impart stretchability to brittle semiconducting polymer thin films (Fig. 1a). Briefly, our TI bonding is enabled by two essential chemical components: (i) a tough self-healing polymer matrix (TSP) capable of repeated energy dissipation through autonomous dynamic bond breakage and reformation, and (ii) a surface modifier (SM) which both covalently and non-covalently bond with the TSP and covalently bond with the substrate (Fig. 1a). This enables a tough interfacial (TI) bonding, prevents delamination, delocalizes strain in the film, and finally significantly delay crack propagation (Fig. 1b). A TSP is composed of a mixture of 90wt% self-healing polymer (SHP) as the energy dissipating matrix and 10 wt% SM as the crosslinker. Specifically, the SHP is a polysiloxane-based tough elastomeric network consisting of two kinds of H (hydrogen)-bonds with different bond strengths. The SM has the following three features: (i) two perfluorophenylazide or benzophenone moieties at the ends of a flexible chain for covalent bonding with any polymer surfaces by light or heat²⁸, (ii) a dynamic H-bonding unit for non-covalent interactions with TSP, and (iii) a flexible long polysiloxane chain (M_w~5000) for stretchability of SM layer (Fig. 1a).

Fig. 2a illustrates the preparation processes of the TI layer. Briefly, we first spin- or dip-coat a solution of SM (5 wt% in isopropanol) on a polymer surface and immobilized SM (7-8 nm)

covalently by UV irradiation for 10 mins and thermal annealing at 150°C for 10 mins. The covalent surface modification was confirmed by X-ray photoelectron spectroscopy (XPS), Fourier-transform infrared spectroscopy (FT-IR) and contact angle measurements (Supplementary Figs 1, 2 and 3). A TSP film (2 µm) composed of a mixture of 90wt% SHP (self-healing polymer, structure shown in Fig. 1a) as the energy dissipating matrix and 10 wt% SM as the crosslinker was laminated onto the SM-modified substrate. Subsequently, the resulting bilayer film was gradually heated to 150°C over 15 mins and annealed for 30 mins to ensure covalent crosslinking. The adhesion energy between the two layers was measured by the 180° peeling test (Figs 2a and 2b)²⁸. The measured values of interfacial fracture energy between TSP and various types of polymer substrates are well over 1,500 J/m², which is much higher than other reported dry adhesives²⁹ (Figs 2a and 2c), indicating tough adhesion between TSP and the substrate.

To further understand the mechanisms for the achieved high interfacial fracture energy, we performed a number of control experiments. First, we observed that without the initial surface modification by SM, the interfacial fracture energy was only 6 J/m² (Supplementary Fig. 4), suggesting that a thin SM layer is essential. Second, the hydrogen bonding moieties in SM structure were observed to be crucial. Without the H-bonds, we observed relatively weak adhesion between TSP and other polymers (Supplementary Fig. 4). Third, when TSP was replaced with a covalently crosslinked PDMS (Sylgard 184) instead of the SHP, the adhesion energy again was low attributed to lack of energy dissipation mechanisms (Fig. 2c). We have previously shown the extremely high stretchablilty and fracture energy of this SHP, where a mixture of strong and weak H-bonds together with highly flexible PDMS chains has been shown to effectively dissipate mechanical energy³⁰ (Supplementary Fig. 5). Therefore, surface covalent bonding of SM combined with bulk dynamic H-bonding for energy dissipation of TSP resulted

in high interfacial toughness. Previous work reported methods to realize high interface toughness with tough hydrogels ^{24,25,27}. This work provides the molecular design for high interface toughness between various non-hydrogel materials. In addition, we confirmed our tough interface (1,300 J/m²) can additionally be realized by benzophenone covalent crosslinkers and energy dissipative polymer matrixes (Supplementary Fig. 4).

To demonstrate the utility of the TI for improving the stretchability of brittle polymer thin films, we applied it first to a well-known high-mobility brittle semiconducting polymer (P1) thin film (40 nm, Fig. 1a). Various multi-layer structures were fabricated, with the dimensions given in Supplementary Fig. 6. Although embedding an interfacial layer between a film and a substrate can function as a buffer layer to hinder fracture, predicted by a shear-lag model³¹, we show that this buffering effect is negligible in our multi-layer structures, given their geometry and material properties (See Methods for more details). To more accurately determine the strain in the semiconducting P1 film, we directly measured it using optical microscope and used it to quantify the crack-onset strain of the film. To determine whether a tough interface between P1 and SM/TSP was indeed achieved, a simple 'scotch-tape test' was performed, in which negligible delamination of the semiconducting layer from SM/TSP (TI) (Supplementary Fig. 7) was observed. Note that the 180° peeling test could not be performed because the semiconducting film typically used for devices are too thin (< 60 nm). In contrast, the transferred P1 on a PDMS substrate, which is typically used for stretchability tests of semiconducting layers, was easily delaminated by the scotch-tape (Supplementary Fig. 7).

A pseudo-freestanding polymer thin film (<100 nm), e.g. a film on water, typically ruptures at a smaller strain than its bulk films (>100 µm), which is attributed to strain localization in the bulk film²⁰. On the other hand, when the thin film (<100 nm) attached on a PDMS substrate is

subjected to strain, multiple smaller cracks, instead of a single complete fracture, were usually observed due to strain delocalization by the polymer substrate (Fig. 1b). For instance, a pseudofreestanding 40 nm P1 and 100 µm thick P1 films completely ruptured at 6% and 16% strain, respectively (Supplementary Fig. 8). In contrast, a P1 film laminated onto a PDMS (P1-PDMS) formed micro-size cracks at 40% strain instead of suffering a complete rupture (Supplementary Fig. 8). Based on this observation and previous theoretical studies²⁰, we hypothesize that if a polymer thin film is strongly bonded to an energy dissipating layer, its strain may be more efficiently delocalized without delamination, and hence crack initiation and propagation can be significantly suppressed or delayed (Supplementary Fig. 9).

To validate our hypothesis, we first measured the crack-onset strain of P1 films with and without a tough interface layer on PDMS (P1-TI-PDMS and P1-PDMS-PDMS, TI = SM/TSP/SM) by optical microscope. As shown in Fig. 3c, we observed a significantly delayed crack-onset strain of P1-TI-PDMS from 40% to 110%, which is also accompanied by a continuously increase in the dichroic ratios via polarized UV-Vis spectroscopy (Supplementary Fig. 10). In addition, we couldn't observe strain-rate dependence on crack-onset strain of P1-TI-PDMS. Even at a high strain rate of 1,000%/min crack-onset strain is significantly delayed in P1-TI-PDMS. (Supplementary Fig. 11).

To further understand the roles of TI, we first investigated the importance of energy dissipation in reducing crack initiation and slowing down crack propagation. Indeed, we observed substantially smaller crack sizes (7 μm to 1.5 μm) and crack numbers in P1-TSP-PDMS (P1 laminated on TSP-PDMS) as compared to those in P1-PDMS-PDMS (P1 laminated on covalently crosslinked PDMS) (Fig. 3a, b, d and Supplementary Fig. 12). In addition, the cracks in P1-TSP-PDMS showed slower propagation upon additional applied strain. Next, relative

degree of crystallinity (RDOC) analysis was used to examine morphological changes of P1 films under strain. The RDOC of P1-PDMS decreased more than that of P1-TSP-PDMS (80% vs. 30%) as tensile strain increased from 0% to 100% (Supplementary Figs 13, 14 and Table 1). We also observed that the measured maximum dichroic ratio for P1-TSP-PDMS is 1.3 times higher than that for P1-PDMS (Supplementary Fig. 10). These results indicate that TSP enhances the bonding between layers and delocalizes strain in the P1 film, preventing crack propagation and breakage of crystalline domains. As a result, high strain induced more alignment of the polymer chains. The mechanism of energy dissipation through dynamic bond breakages within the semiconducting thin film has been previously observed to improve its intrinsic stretchability¹⁵, and increase interface adhesion²⁶. Here, we confirm that the energy dissipating interface layer can be used to enable improved bonding, delay crack initiation and propagation in brittle polymer thin films.

Next, the effect of covalent bonding given by SM treatment was investigated. We observed delayed crack-onset strain for P1-SM-PDMS from 40% to 60% strain (Fig. 3c). Notably, at crack-onset strain, P1-SM-PDMS showed lower crack density compared to that for P1-PDMS, indicating that the improved adhesion delayed crack initiation and propagation. This effect is more noticeable after 100 stress-strain cycles with 50% strain. As shown in Fig. 3e, P1-PDMS exhibits a substantial increase in crack sizes and density compared to P1-SM-PDMS (Fig. 3e and Supplementary Fig. 15). To exclude the possibility of microstructural changes of P1 caused by SM treatment, UV-vis spectroscopy and GIXD measurements were performed, which confirmed no observable changes in P1 aggregation behavior and microstructures (Supplementary Fig. 16).

Next, we investigate the effect of thickness of a polymer semiconducting film on its crack

initiation and propagation in presence of TI. As films get thicker, they are expected to behave more like the bulk materials. As shown in Supplementary Fig. 17, even for a 100 nm P1 film, the effect of TI on fracture behaviors is still present. The crack sizes in P1 (~125 nm)-TI-PDMS were 5 times smaller than those in P1 (~125 nm)-PDMS at the crack onset strain (Supplementary Fig. 17).

We further observed that TI stabilized stress-strain cycles as well as thermal cycles. Specifically, due to the plastic nature of P1 semiconducting films, wrinkle formation without delamination was observed for P1-TI after released from 100% strain (Supplementary Fig. 18). Wrinkle structures have been used as a strategy to achieve macroscopic reversible stretchability and provide an additional mechanism for stable stretching cycles for P1-TI films. In addition, we observed an improved thermal stability of P1-TI with no change of crack onset strain after thermal annealing at 100 °C for 10 minutes and no noticeable cracks even at 100% strain while P1-PDMS crack onset strain reduced to 20% (Supplementary Fig. 19).

To better explain the mechanisms for TI design, we theoretically investigated the toughening mechanism of P1-TI-PDMS. Since it has been well established that energy dissipation in a hydrogel and its covalent bonding to another material are important in enhancing the interfacial toughness ^{25,26}, we assume the bonding between layers in P1-TI-PDMS is strong enough so that no delamination occurs. This way, we focus on investigating the effect of the substrate and TI layer in delaying crack propagation. P1 is modeled as a power-law material (See Methods for more details; Supplementary Fig. 20), which can be predicted to form necking at 3% strain when free standing, and subsequently rupture with a single crack. However, when stretching P1-TI-PDMS, necking localization was observed to be prevented. We conducted 2D finite element simulations to compute the energy release rates of a multi-layer structure of P1-TI-PDMS

subjected to external strain (See Methods for more details; Figs 3f, 3g and Supplementary Fig. 21). As a comparison, the energy release rates for P1-SM-PDMS were also computed under the assumption of no delamination to estimate an upper bound of the critical strain for crack propagation, while delamination can produce a lower critical strain. Both TI and PDMS are modeled as Arruda-Boyce materials²⁴. The steady state energy release rate G_{ss} as a function of strain ε is computed (See Methods for more details; Fig. 3f). Considering typical fracture energy Γ of polymer semiconducting thin films is on the order of 10 J/m^{2 32}, our simulations predict that a semiconducting thin film bonded perfectly to a substrate can survive a strain ε_c above 100% by using the condition $G_{ss}(\varepsilon_c) = \Gamma$ (Fig. 3g). This indicates that a semiconducting thin film firmly bonded to a substrate can be stretchable. Moreover, the energy release rate G_{ss} of P1-TI-PDMS is always lower than that of P1-SM-PDMS due to the higher stiffness of TI than PDMS, indicating that the addition of the TI layer can delay crack propagation by not only strengthening the interfacial adhesion, but also reducing the crack opening through more strongly constraining the deformation of P1.

Finally, to study the electrical performance of stretchable P1 film enabled by TI design, we proceed to fabricate a fully stretchable transistor in a bottom-gate-top-contact structure, with spray-coated carbon nanotube (CNT) networks as the electrodes, a 2.1 μm TI layer as the dielectric layer and a 100 μm PDMS (Sylgard 184) film as the elastic substrate (Supplementary Fig. 22). The obtained devices exhibited standard field-effect transistor characteristics and an average mobility of 0.73 (+/- 0.14) cm²/V·s from 9 devices (Supplementary Fig. 23). At 100% strain along the current flow direction, the calculated average mobility after correcting for the changes of channel length and dielectric capacitance was still maintained at ~0.53 (+/- 0.16) cm²/V·s even under 100% strain (Fig. 3c, Supplementary Fig. 24 and Supplementary Table 2). In addition, after 100 repeated stretching cycles at 0-50% strain, there was only a small change

in the on-current after the second stretch-and-release cycle, which was attributed to wrinkle formation of P1-TI bilayer without delamination after the first stretch-and-release process (Fig. 4e and Supplementary Fig. 24). In comparison, when a 2 µm-thick covalently crosslinked PDMS, instead of the tough interface layer, was used as the dielectric layer, a significant drop in the on-current was observed immediately after being stretched to 50% strain (Supplementary Fig. 24). Furthermore, microcracks in P1 upon stretching were observed.

The TI layer designed here is applicable to most semiconducting polymers. As an example, we applied it to three additional semiconducting polymers (Fig. 4a). All the thin films directly transferred on a stretchable covalently crosslinked PDMS substrate severely cracked when subjected to 50% strain. But with a TI layer between the semiconducting films and the substrate again delayed crack initiation and propagation, so that we could not observe noticeable cracks even at 100% stain (Figs 4a and 4b). TI can also be used to enhance stretchability of other types of electronic materials. For example, a conducting polymer (PEDOT:PSS) thin film, which exhibits brittle fracture at 10% strain when deposited on a PDMS substrate³³, shows stable conductivity even under 100% strain with the TI layer (Figs 4c, 4d and Supplementary Fig. 25). Similarly, TI can be introduced to a thin gold film (60 nm thick) on a PDMS substrate (Supplementary Fig. 26). The film was observed to change from brittle to ductile fracture, resulting in a stretchable gold conductor (Figs 4e and 4f)³³. Taken together, our work suggest that TI approach may open new avenues for future developments of stretchable electronics by broadening materials choices.

Acknowledgments

This work is supported by Samsung Electronics. J.M acknowledges Samsung Scholarship for financial support. L.J. acknowledges the support from the National Science Foundation through Grant No. CMMI-1925790. J.K acknowledges the support from the National Research Foundation of Korea through Grant No. 2021R1C1C1011116. The authors acknowledge Prof. John Hutchinson of Harvard University for the insightful discussions. Part of this work was performed at the Stanford Nano Shared Facilities (SNSF).

Author Contributions

J.K, J.M, and Z.B conceived concept and designed the experiments. J.K synthesized and characterized the molecules and polymers. Y.Z provided the conjugated polymers. J.K, J.M. and Y.Z designed the device experiments and evaluated the stretchability of materials and devices. J.K and J.M fabricated the fully stretchable OTFTs. M.K and L.J performed the mechanical simulations. J.M and H.W performed the grazing incidence X-ray diffraction experiments and analysis. S.C performed the XPS. J.K, J.M, M.K, J.B.-H.T., L.J and Z.B. wrote the paper.

Competing Interests

The authors declare no competing interests.

Fig. 1. Introducing a tough interface between a semiconducting film and an elastic substrate. **a,** Schematic representation of a tough interface (TI) between a semiconducting film and an elastic substrate. The tough interface bonding is enabled by two essential chemical components: (i) a surface modifier (SM) and (ii) siloxane-based self-healing polymer (SHP) capable of self-recoverable energy dissipation. A tough self-healing polymer (TSP) is composed of a mixture of 90wt% SHP as the energy dissipating matrix and 10 wt% SM as the crosslinker. **b,** Schematic representation of fracture conditions of a polymer thin film under various conditions. Under the free-standing condition, a polymer thin film undergoes brittle fracture separated into two pieces by stretching. When the thin film is attached onto an elastic polymer substrate, microcracks form in the polymer thin film instead of complete fracture. This work shows that embedding a TI layer delays crack initiation and propagation.

Fig. 2. Fabrication and characterization of tough interface between TSP and various polymer substrates. **a,** Schematic of the fabrication procedure for the tough interface. An elastomer substrate (200 μm) was surface modified by SM (7 nm). Then, TSP film (200 μm, 90wt% SHP+10wt% SM) was laminated and annealed at 150 °C for 1 hour. **b,** The measured peeling forces per width of the substrate as functions of the applied displacement for different types of interfaces. (Strain rate: 200%/min). The black arrows indicate the effect of covalent interface crosslinking. The red arrow indicates the effect of energy dissipation. **c,** Summary of the measured interfacial toughness of various elastomer/TI and elastomer/TSP. SM could not be covalently fixed onto PTFE due to lack of CH₂ groups, resulting in poor adhesion. The error bars describe the standard error for three samples in each case.

Fig. 3. Delayed crack formation in semiconducting thin films through embedding a tough interface. **a,** Schematic illustrations of semiconducting thin films on an elastic PDMS substrate with various interface conditions **b,** Optical microscope images of (i) (left) and (iv) (right) at 100% strain. **c,** Summary of crack onset strains of P1 films with various interface conditions shown in (**a**); the error bars represent the results from three batches of samples. **d,** Histograms of the crack lengths in P1 films with condition (i) (black) and (ii) (orange) under 40% (top) and 60% (bottom) strains. Data were collected from 5 images for each condition. We confirmed the effect of energy dissipation of TI on delaying crack initiation and propagation. **e,** Histograms of the crack lengths in P1 films with condition (i) (black) and (iii) (green) under 60% strain

(top) and after 100 stretching cycles under 60% strain (bottom). Data were collected from 5 images for each condition. We confirmed the effect of covalent bonding on delaying crack initiation and propagation. **f**, The finite element simulations to compute the energy release rate for a steady-state channel crack of P1 in P1-TI-PDMS and P1-SM-PDMS multi-layer structures, with the zoom-in view showing the simulation result and definition of the crack opening displacement $\delta(y)$. **g**, The calculated steady-state energy release rate G_{ss} (J/m²) as a function of strain (%) for P1-TI-PDMS and P1-SM-PDMS.

Fig. 4. Broad applicability of the tough interface to various polymer semiconductors and conductors. **a,** Optical microscope images of Px-PDMS (top) and Px-TI (bottom) (x=2, 3, 4) at 50% strain. **b,** Summary of crack onset strains of Px films (x=1, 2, 3, 4) with respect to various interface conditions. **c,** Optical microscope images of stretched PEDOT:PSS films: PEDOT:PSS on PDMS at 20% strain (left), PEDOT:PSS on TI at 40% (middle) and 80% (right) strain. PEDOT:PSS film was directly spin coated on oxygen plasma treated-PDMS and -TSP. **d,** Electrical resistance changes of PEDOT:PSS film during stretching. The width, length, and thickness of the sample are 0.5 cm, 2 cm, and 50 nm, respectively. **e,** Optical microscope images of Au films on PDMS (top) and TSP (bottom) at 0% strain (left) and 50% strain (right), respectively. **f.** Electrical resistance changes of Au films during stretching. (Scale bar: 20 μm) The width, length, and thickness of the sample are 0.5 cm, 2 cm, and 60 nm, respectively.

References

- 1. Someya, T., Bao, Z. & Malliaras, G. G. The rise of plastic bioelectronics. *Nature* **540**, 379–385 (2016).
- 2. Miyamoto, A., Lee, S., Cooray, N. F., Lee, S., Mori, M., Matsuhisa, N., Jin, H., Yoda, L., Yokota, T., Itoh, A., Sekino, M., Kawasaki, H., Ebihara, T., Amagai, M. & Someya, T. Inflammation-free, gas-permeable, lightweight, stretchable on-skin electronics with nanomeshes. *Nat. Nanotechnol.* **12,** 907–913 (2017).
- 3. Kang, J., Tok, J. B. H. & Bao, Z. Self-healing soft electronics. *Nat. Electron.* **2**, 144–150 (2019).
- 4. Park, S., Heo, S. W., Lee, W., Inoue, D., Jiang, Z., Yu, K., Jinno, H., Hashizume, D., Sekino, M., Yokota, T., Fukuda, K., Tajima, K. & Someya, T. Self-powered ultra-

- flexible electronics via nano-grating-patterned organic photovoltaics. *Nature* **561**, 516–521 (2018).
- 5. Kaltenbrunner, M., Sekitani, T., Reeder, J., Yokota, T., Kuribara, K., Tokuhara, T., Drack, M., Schwödiauer, R., Graz, I., Bauer-Gogonea, S., Bauer, S. & Someya, T. An ultra-lightweight design for imperceptible plastic electronics. *Nature* **499**, 458–463 (2013).
- 6. Wagner, S. & Bauer, S. Materials for stretchable electronics. *MRS Bull.* **37**, 207–213 (2012).
- 7. Chortos, A., Liu, J. & Bao, Z. Pursuing prosthetic electronic skin. *Nat. Mater.* **15,** 937–950 (2016).
- 8. Lee, S., Sasaki, D., Kim, D., Mori, M., Yokota, T., Lee, H., Park, S., Fukuda, K., Sekino, M., Matsuura, K., Shimizu, T. & Someya, T. Ultrasoft electronics to monitor dynamically pulsing cardiomyocytes. *Nat. Nanotechnol.* (2018). doi:10.1038/s41565-018-0331-8
- 9. Wang, S., Oh, J. Y., Xu, J., Tran, H. & Bao, Z. Skin-Inspired Electronics: An Emerging Paradigm. *Acc. Chem. Res.* **51**, 1033–1045 (2018).
- 10. Wang, S., Xu, J., Wang, W., Wang, G. J. N., Rastak, R., Molina-Lopez, F., Chung, J. W., Niu, S., Feig, V. R., Lopez, J., Lei, T., Kwon, S. K., Kim, Y., Foudeh, A. M., Ehrlich, A., Gasperini, A., Yun, Y., Murmann, B., Tok, J. B. H. & Bao, Z. Skin electronics from scalable fabrication of an intrinsically stretchable transistor array. *Nature* 555, 83–88 (2018).
- 11. Yang, J. C., Mun, J., Kwon, S. Y., Park, S., Bao, Z. & Park, S. Electronic Skin: Recent Progress and Future Prospects for Skin-Attachable Devices for Health Monitoring, Robotics, and Prosthetics. *Adv. Mater.* **31**, 1904765 (2019).
- 12. Kim, D.-H., Ahn, J.-H., Choi, W. M., Kim, H.-S., Kim, T.-H., Song, J., Huang, Y. Y., Liu, Z., Lu, C. & Rogers, J. A. Stretchable and Foldable Silicon Integrated Circuits. *Science* (80-.). **320**, 507–511 (2008).
- 13. Kim, D.-H., Lu, N., Ma, R., Kim, Y.-S., Kim, R.-H., Wang, S., Wu, J., Won, S. M., Tao, H., Islam, A., Yu, K. J., Kim, T. -i., Chowdhury, R., Ying, M., Xu, L., Li, M., Chung, H.-J., Keum, H., McCormick, M., Liu, P., Zhang, Y.-W., Omenetto, F. G., Huang, Y., Coleman, T. & Rogers, J. A. Epidermal Electronics. *Science (80-.)* 333, 838–843 (2011).
- 14. Root, S. E., Savagatrup, S., Printz, A. D., Rodriquez, D. & Lipomi, D. J. Mechanical

- Properties of Organic Semiconductors for Stretchable, Highly Flexible, and Mechanically Robust Electronics. *Chem. Rev.* **117**, 6467–6499 (2017).
- 15. Oh, J. Y., Rondeau-Gagné, S., Chiu, Y. C., Chortos, A., Lissel, F., Wang, G. J. N., Schroeder, B. C., Kurosawa, T., Lopez, J., Katsumata, T., Xu, J., Zhu, C., Gu, X., Bae, W. G., Kim, Y., Jin, L., Chung, J. W., Tok, J. B. H. & Bao, Z. Intrinsically stretchable and healable semiconducting polymer for organic transistors. *Nature* **539**, 411–415 (2016).
- Mun, J., Wang, G. N., Oh, J. Y., Katsumata, T., Lee, F. L., Kang, J., Wu, H., Lissel, F., Rondeau-Gagné, S., Tok, J. B.-H. & Bao, Z. Effect of Nonconjugated Spacers on Mechanical Properties of Semiconducting Polymers for Stretchable Transistors. *Adv. Funct. Mater.* 28, 1804222 (2018).
- 17. Zheng, Y., Wang, G. N., Kang, J., Nikolka, M., Wu, H., Tran, H., Zhang, S., Yan, H., Chen, H., Yuen, P. Y., Mun, J., Dauskardt, R. H., McCulloch, I., Tok, J. B. -H., Gu, X. & Bao, Z. An Intrinsically Stretchable High-Performance Polymer Semiconductor with Low Crystallinity. *Adv. Funct. Mater.* **29**, 1905340 (2019).
- 18. Zheng, Y., Zhang, S., Tok, J. B. H. & Bao, Z. Molecular Design of Stretchable Polymer Semiconductors: Current Progress and Future Directions. *J. Am. Chem. Soc.* **144**, 4699–4715 (2022).
- 19. Xu, J., Wang, S., Wang, G.-J. N., Zhu, C., Luo, S., Jin, L., Gu, X., Chen, S., Feig, V. R., To, J. W. F., Rondeau-Gagné, S., Park, J., Schroeder, B. C., Lu, C., Oh, J. Y., Wang, Y., Kim, Y., Yan, H., Sinclair, R., Zhou, D., Xue, G., Murmann, B., Linder, C., Cai, W., Tok, J. B.-H., Chung, J. W. & Bao, Z. Highly stretchable polymer semiconductor films through the nanoconfinement effect. *Science* (80-.). 355, 59–64 (2017).
- 20. Suo, Z., Vlassak, J. & Wagner, S. Micromechanics of macroelectronics. *China Particuology* **3**, 321–328 (2005).
- 21. Xiang, Y., Li, T., Suo, Z. & Vlassak, J. J. High ductility of a metal film adherent on a polymer substrate. *Appl. Phys. Lett.* **87**, 161910 (2005).
- 22. Lu, N., Wang, X., Suo, Z. & Vlassak, J. Metal films on polymer substrates stretched beyond 50%. *Appl. Phys. Lett.* **91,** 221909 (2007).
- 23. Lee, S.-Y., Park, K. R., Kang, S., Lee, J., Jeon, E., Shim, C., Ahn, J., Kim, D.-I., Han, H. N., Joo, Y., Kim, C. & Choi, I. Selective crack suppression during deformation in metal films on polymer substrates using electron beam irradiation. *Nat. Commun.* 10, 4454 (2019).

- 24. Yang, J., Bai, R. & Suo, Z. Topological Adhesion of Wet Materials. *Adv. Mater.* **30,** 1–7 (2018).
- 25. Liu, Q., Nian, G., Yang, C., Qu, S. & Suo, Z. Bonding dissimilar polymer networks in various manufacturing processes. *Nat. Commun.* **9,** 1–11 (2018).
- 26. Yuk, H., Zhang, T., Lin, S., Parada, G. A. & Zhao, X. Tough bonding of hydrogels to diverse non-porous surfaces. *Nat. Mater.* **15**, 190–196 (2016).
- 27. Yuk, H., Zhang, T., Parada, G. A., Liu, X. & Zhao, X. Skin-inspired hydrogel-elastomer hybrids with robust interfaces and functional microstructures. *Nat. Commun.* **7,** 1–11 (2016).
- 28. Wang, G. N., Zheng, Y., Zhang, S., Kang, J., Wu, H., Gasperini, A., Zhang, H., Gu, X. & Bao, Z. Tuning the Cross-Linker Crystallinity of a Stretchable Polymer Semiconductor. *Chem. Mater.* **31**, 6465–6475 (2019).
- 29. Lee, H., Lee, B. P. & Messersmith, P. B. A reversible wet/dry adhesive inspired by mussels and geckos. *Nature* **448**, 338–341 (2007).
- 30. Kang, J., Son, D., Wang, G. J. N., Liu, Y., Lopez, J., Kim, Y., Oh, J. Y., Katsumata, T., Mun, J., Lee, Y., Jin, L., Tok, J. B. H. & Bao, Z. Tough and Water-Insensitive Self-Healing Elastomer for Robust Electronic Skin. *Adv. Mater.* **30**, 1–8 (2018).
- 31. Sun, J. Y., Lu, N., Yoon, J., Oh, K. H., Suo, Z. & Vlassak, J. J. Inorganic islands on a highly stretchable polyimide substrate. *J. Mater. Res.* **24**, 3338–3342 (2009).
- 32. Zhang, S., Koizumi, M., Cao, Z., Mao, K. S., Qian, Z., Galuska, L. A., Jin, L. & Gu, X. Directly Probing the Fracture Behavior of Ultrathin Polymeric Films. *ACS Polym. Au* 1, 16–29 (2021).
- 33. Wang, Y., Zhu, C., Pfattner, R., Yan, H., Jin, L., Chen, S., Molina-Lopez, F., Lissel, F., Liu, J., Rabiah, N. I., Chen, Z., Chung, J. W., Linder, C., Toney, M. F., Murmann, B. & Bao, Z. A highly stretchable, transparent, and conductive polymer. *Sci. Adv.* 3, 1–11 (2017).

Methods

Sample preparation. P1-X-X' means that P1 film is on X' substrate with X interface layer. For SM, we used perfluoroazide version (SM-1) for most of experiments. We also designed SM-2 (benzophenone version), which can readily crosslink with almost any surfaces with C-H bonds as another universal crosslinker.

Px-PDMS-PDMS: a polymer semiconductor film (Px, 40 nm) was were prepared on OTS-treated SiO₂. A PDMS layer (2 μ m) was directly spin-coated on Px from a PDMS solution (5 g Sylgard 184-precursor: crosslinker = 15:1 in 20 mL hexane) at 2000 rpm for 2 min. After annealing at 150 °C for an hour, the resulting film was transferred onto another crosslinked PDMS substrates (Precursor: Crosslinker = 20:1, thickness 200 μ m).

Px-SM-PDMS: a polymer semiconductor film (Px, 40 nm) was prepared on OTS-treated SiO₂. SM solution in hexane (5wt%) was first spin-coated at 3,000 rpm for 1 min onto the polymer film was annealed at 150 °C for an hour. The resulting film was transferred onto crosslinked PDMS substrates (Precursor: Crosslinker = 20:1, thickness 200 μ m).

Px-TI-PDMS: a polymer semiconductor film (Px, 40 nm) was prepared on OTS-treated SiO₂. SM solution in hexane (5wt%) was first spin-coated at 3,000 rpm for 1 min onto the polymer film was annealed at 150 °C for an hour. Subsequently, SHP/SM (90/10, wt/wt ratio) solution (100 mg/ml) in hexane/IPA (95/5, v/v) was directly spin-coated onto polymer film-SM was annealed again at 150°C for an hour. The resulting film was transferred onto crosslinked PDMS substrates (Precursor: Crosslinker = 20:1, thickness 200 μm).

Fully Stretchable Transistor Fabrication. For gate electrodes, CNT (P2-SWNT, Carbon Solutions Inc.) and Poly(3-hexylthiophene-2,5-diyl) (P3HT) were dispersed in chloroform (0.2 mg mL⁻¹ CNT and 0.05 mg mL⁻¹ P3HT). Ultrasonication of the CNT/P3HT/chloroform mixture was conducted for 30 minutes at 30% amplitude using a 750 W ultrasonication probe. Centrifugation of the ultrasonicated solution at 8,000 rpm for 30 minutes resulted in a welldispersed CNT solution in chloroform. The CNT supernatant solution was spray-coated on an OTS-treated SiO₂ wafer using a commercially available airbrush (Master Airbrush, SB844). The spray-coated CNT layer (~ 40 nm) was embedded into SHP (PDMS-MPU_{0.3}-IU_{0.7}) (2 μm thickness) and subsequently transferred to a PDMS substrates (Precursor: Crosslinker = 15:1, 150 µm thickness). A semiconducting polymer solution was spin-coated on an OTS-treated SiO₂ wafer at 1,500 rpm for 1 minute. The thin film (40 nm) was annealed at 150 °C for 30 minutes. SM (5wt% in Hexane) was directly spin-coated onto the annealed polymer thin films at 2,000 rpm for 1 minute and subsequently annealed at 150 °C for an hour. Next, the dielectric layer (i.e. TI layer) was prepared by directly spin-coating a TSP solution (80 mg mL⁻¹, SHP:SM = 9:1 wt/wt in hexane/IPA = 10/1 v/v) onto the annealed polymer semiconductor thin film. The thickness of the dielectric layer was around 2.1 µm. The semiconductor-TI film on OTS-treated SiO₂ was further annealed at 80 °C overnight. Next, it was directly transferred onto the gate/substrate. For source/drain electrodes, CNT (P3-SWNT, Carbon Solutions Inc.) was dispersed in isopropanol (IPA). First, 0.3 mg mL⁻¹ CNT/IPA solution was bath sonicated for 4 hours. Then, the solution was ultrasonicated for 30 minutes at 30% amplitude using a 750 W ultrasonication probe. The as-dispersed CNT solution was centrifugated at 6,000 rpm for 30 minutes. Finally, the well-dispersed CNT supernatant was directly spray-coated onto the semiconductor layer using a commercial air brush (Master Airbrush, SB844) and patterned through a metal shadow mask with the channel length of 150 µm and the channel width of 1,000 μm.

Film Characterization. Crack onset strain was measured using "film-on-elastomer" methods for various thin films. Crack onset was determined with an optical microscope. In our experiments, we measured the actual applied strain to the semiconducting film and used it to

determine crack-onset strain of film to avoid the different strain distribution problems caused by interface layer. Thin film UV-Vis spectroscopy was performed with Agilent Cary 6000i UV-vis-NIR spectrometer. GIXD experiments were conducted at beamline 11-3 of Stanford Synchrotron Radiation Lightsource (SSRL). Electrical characterizations of transistors and conductivity were carried out with Keithley 4200 parameter analyzer.

Finite Element Simulations. We calculated the steady-state energy release rate of channel crack in a P1 film in P1-TI-PDMS and P1-SM-PDMS, respectively, via finite element analysis using ABAQUS finite element package. We first built 2D simulation models for P1-TI-PDMS and P1-SM-PDMS multi-layer structures with a channel pre-crack in the P1 film, assuming no delamination between all the layers (Fig. 3f). We also built 3D simulation models, but the energy release rate for steady-state crack propagation was similar to that of 2D, so here we only present the results from 2D simulations. The geometric dimensions and symmetric boundary conditions of P1-TI-PDMS are shown in Supplementary Fig. 18a. For P1-SM-PDMS, the TI layer is simply omitted. The P1 film is modeled as a power-law material

ε

$$= \frac{\sigma}{E} \left(1 + \alpha \left(\frac{\sigma}{\sigma_y} \right)^{n-1} \right),\tag{1}$$

with the material law implemented to ABAQUS by fitting the experimental stress-strain curve to a Marlow free energy. In Eq. 1, ε is the strain, σ is the stress, the Young's modulus E is fitted to the experimental measurement to be 600 MPa, the yield strength is fitted to be $\sigma_y = 6$ MPa, the yield offset $\alpha = 0.001$, and the hardening exponent n = 20. Both TI and PDMS are modeled as Arruda-Boyce materials, with the shear modulus $\mu = 2.4$ MPa and 0.150 MPa, respectively, and stretch limit $\lambda_m = 9$ and 2.4, respectively. We deformed the multi-layer structures to external strain ε using displacement control, and computed the remote stress distribution $\sigma(y)$ across the film thickness, and the crack opening displacement distribution $\delta(y)$ (Fig. 3f). Then we can use the following formula to calculate the steady-state energy release rate G_{ss} as a function of ε

$$G_{ss} = \frac{1}{2h} \int_0^h \sigma(y) \, \delta(y) dy, \tag{2}$$

with h the film thickness^{34,35}. By comparing the steady-state energy release rate G_{ss} with the fracture energy of P1, Γ , $G_{ss}(\varepsilon_c) = \Gamma$, we can determine the critical strain for steady-state crack propagation ε_c .

Shear-lag model. Using a shear-lag model, we can estimate the maximal strain in P1, ε_{max} , when strain ε_{app} is applied to the PDMS substrate in P1-TI-PDMS³²

$$\frac{\varepsilon_{max}}{\varepsilon_{app}} = 1 - \frac{1}{\cosh\left(\frac{L}{2\Lambda}\right)},\tag{3}$$

where

$$\Lambda = \sqrt{\frac{E_{P1}h_{P1}h_{TI}}{\mu_{TI}}},\tag{4}$$

with E_{P1} and h_{P1} the Young's modulus and thickness of P1, and μ_{TI} and h_{TI} the shear modulus and thickness of TI, and L the length of the multi-layer structure. Given that $E_{P1} = 600$ MPa, $h_{P1} = 50$ nm, $\mu_{TI} = 2.4$ MPa, $h_{TI} = 2$ μm , and L = 1.5 cm, we can estimate $\Lambda = 5$ μm , and ϵ_{max} is almost equal to ϵ_{app} .

Data Availability

The authors declare that the main data supporting the findings of this study are available within the article and its Supplementary Information. Supplementary information is available in the online version of the paper. Reprints and permissions information is available online at www.nature.com/reprints. Correspondence and requests for materials should be addressed to Z.B.

Methods-only References

- 34. Ambrico, J. M. & Begley, M. R. The role of initial flaw size, elastic compliance and plasticity in channel cracking of thin films. *Thin Solid Films* **419**, 144–153 (2002).
- 35. Beuth, J. L. & Klingbeil, N. W. Cracking of thin films bonded to elastic plastic substrates. *J. Mech. Phys. Solids* **44**, 1411–1428 (1996).

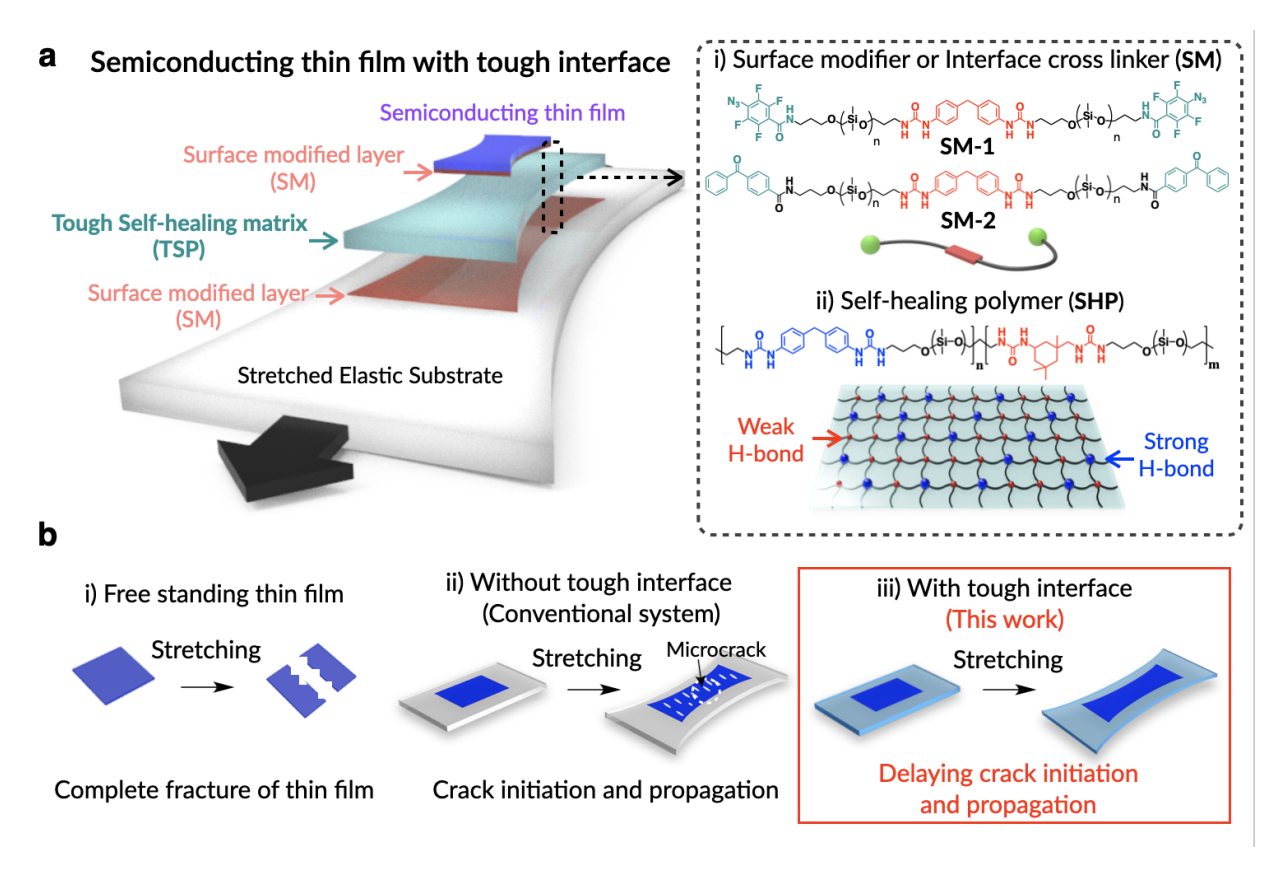


Fig. 1. Introducing a tough interface between a semiconducting film and an elastic substrate. **a,** Schematic representation of a tough interface (TI) between a semiconducting film and an elastic substrate. The tough interface bonding is enabled by two essential chemical components: (i) a surface modifier (SM) and (ii) siloxane-based self-healing polymer (SHP) capable of self-recoverable energy dissipation. A tough self-healing polymer (TSP) is composed of a mixture of 90wt% SHP as the energy dissipating matrix and 10 wt% SM as the crosslinker. **b,** Schematic representation of fracture conditions of a polymer thin film under various conditions. Under the free-standing condition, a polymer thin film undergoes brittle fracture separated into two pieces by stretching. When the thin film is attached onto an elastic polymer substrate, microcracks form in the polymer thin film instead of complete fracture. This work shows that embedding a TI layer delays crack initiation and propagation.

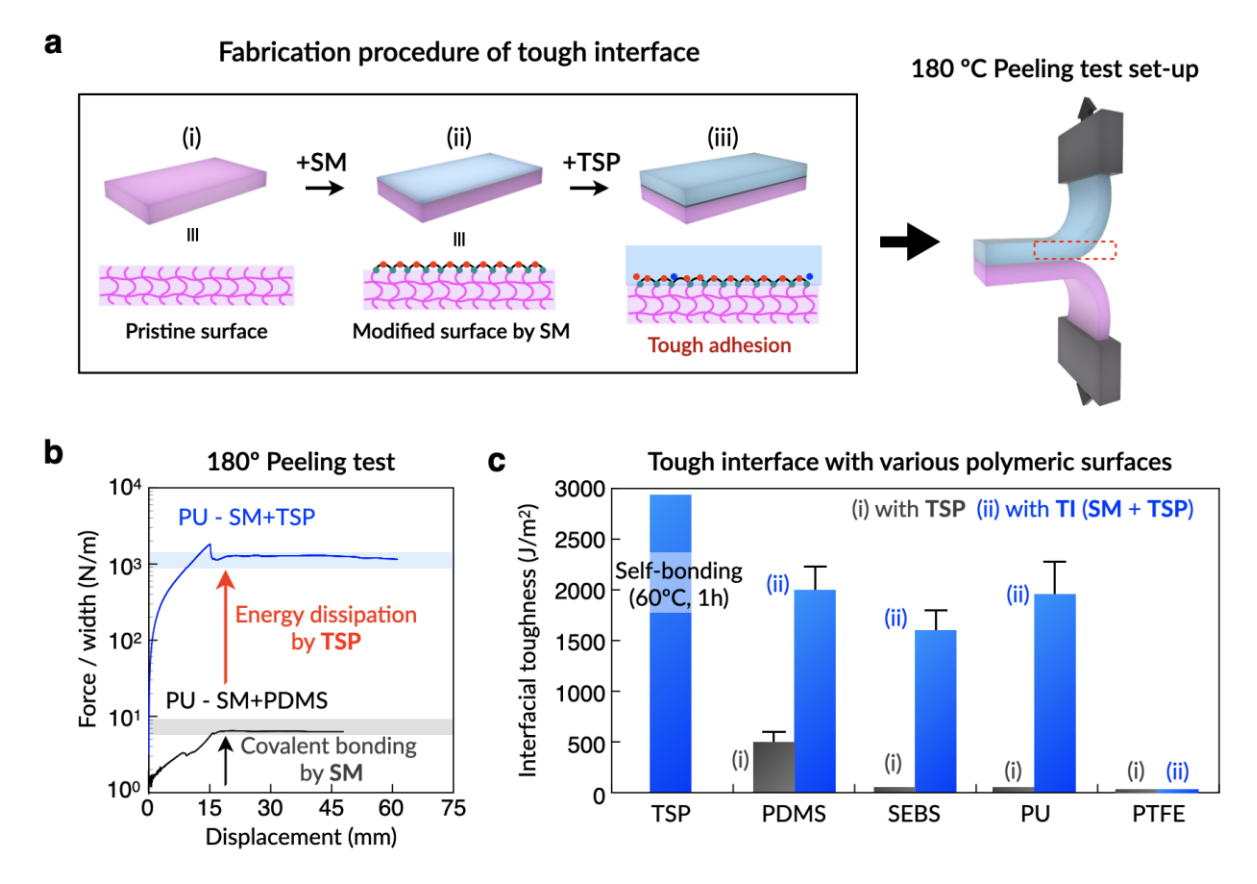


Fig. 2. Fabrication and characterization of tough interface between TSP and various polymer substrates. **a,** Schematic of the fabrication procedure for the tough interface. An elastomer substrate (200 μm) was surface modified by SM (7 nm). Then, TSP film (200 μm, 90wt% SHP+10wt% SM) was laminated and annealed at 150 °C for 1 hour. **b,** The measured peeling forces per width of the substrate as functions of the applied displacement for different types of interfaces. (Strain rate: 200%/min). The black arrows indicate the effect of covalent interface crosslinking. The red arrow indicates the effect of energy dissipation. **c,** Summary of the measured interfacial toughness of various elastomer/TI and elastomer/TSP. SM could not be covalently fixed onto PTFE due to lack of CH₂ groups, resulting in poor adhesion.

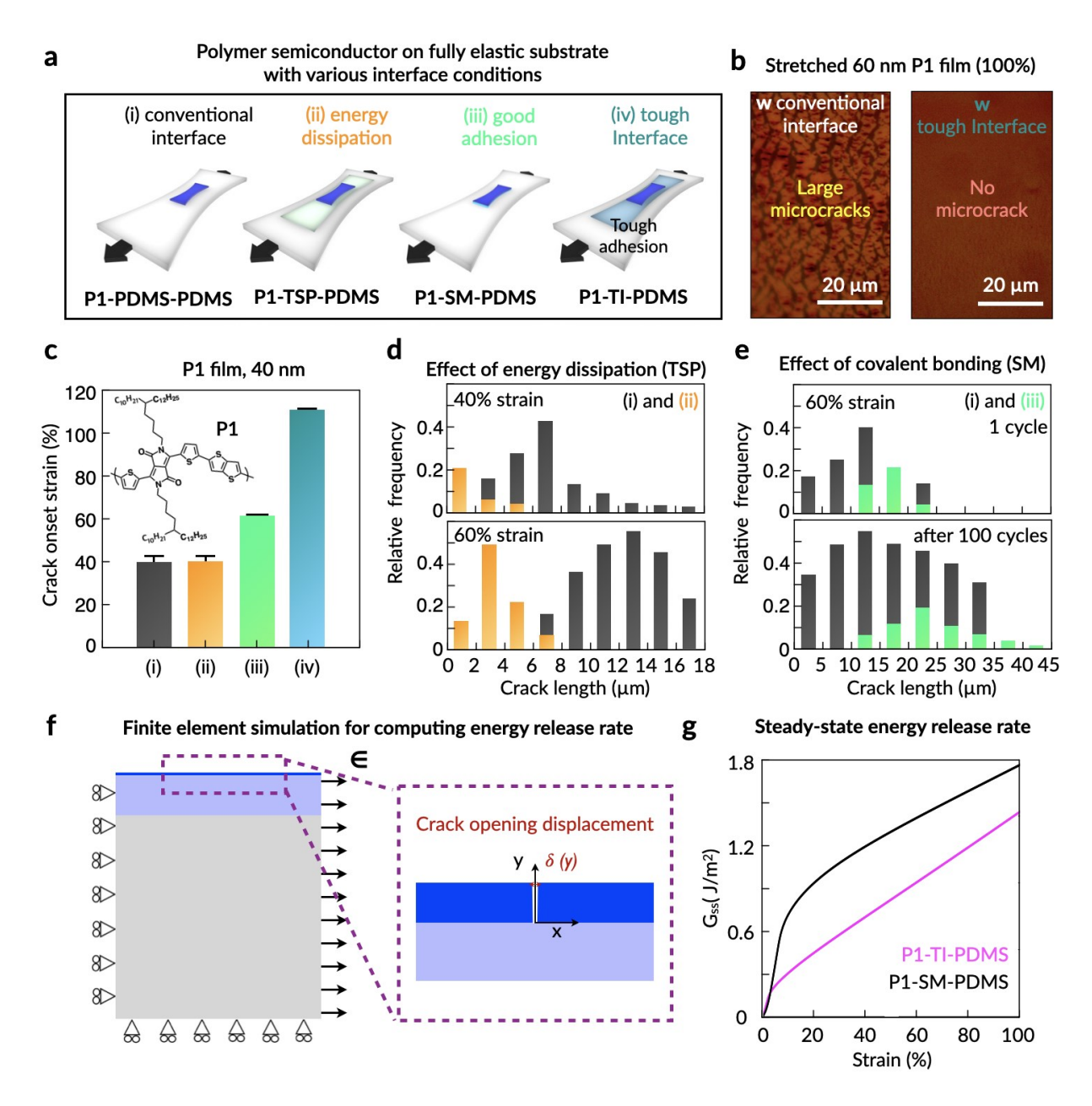


Fig. 3. Delayed crack formation in semiconducting thin films through embedding a tough interface. **a,** Schematic illustrations of semiconducting thin films on an elastic PDMS substrate with various interface conditions **b,** Optical microscope images of (i) (left) and (iv) (right) at 100% strain. **c,** Summary of crack onset strains of P1 films with various interface conditions shown in (**a**); the error bars represent the results from three batches of samples. **d,** Histograms of the crack lengths in P1 films with condition (i) (black) and (ii) (orange) under 40% (top) and

60% (bottom) strains. Data were collected from 5 images for each condition. We confirmed the effect of energy dissipation of TI on delaying crack initiation and propagation. **e**, Histograms of the crack lengths in P1 films with condition (i) (black) and (iii) (green) under 60% strain (top) and after 100 stretching cycles under 60% strain (bottom). Data were collected from 5 images for each condition. We confirmed the effect of covalent bonding on delaying crack initiation and propagation. **f**, The finite element simulations to compute the energy release rate for a steady-state channel crack of P1 in P1-TI-PDMS and P1-SM-PDMS multi-layer structures, with the zoom-in view showing the simulation result and definition of the crack opening displacement $\delta(y)$. **g**, The calculated steady-state energy release rate G_{ss} (J/m²) as a function of strain (%) for P1-TI-PDMS and P1-SM-PDMS.

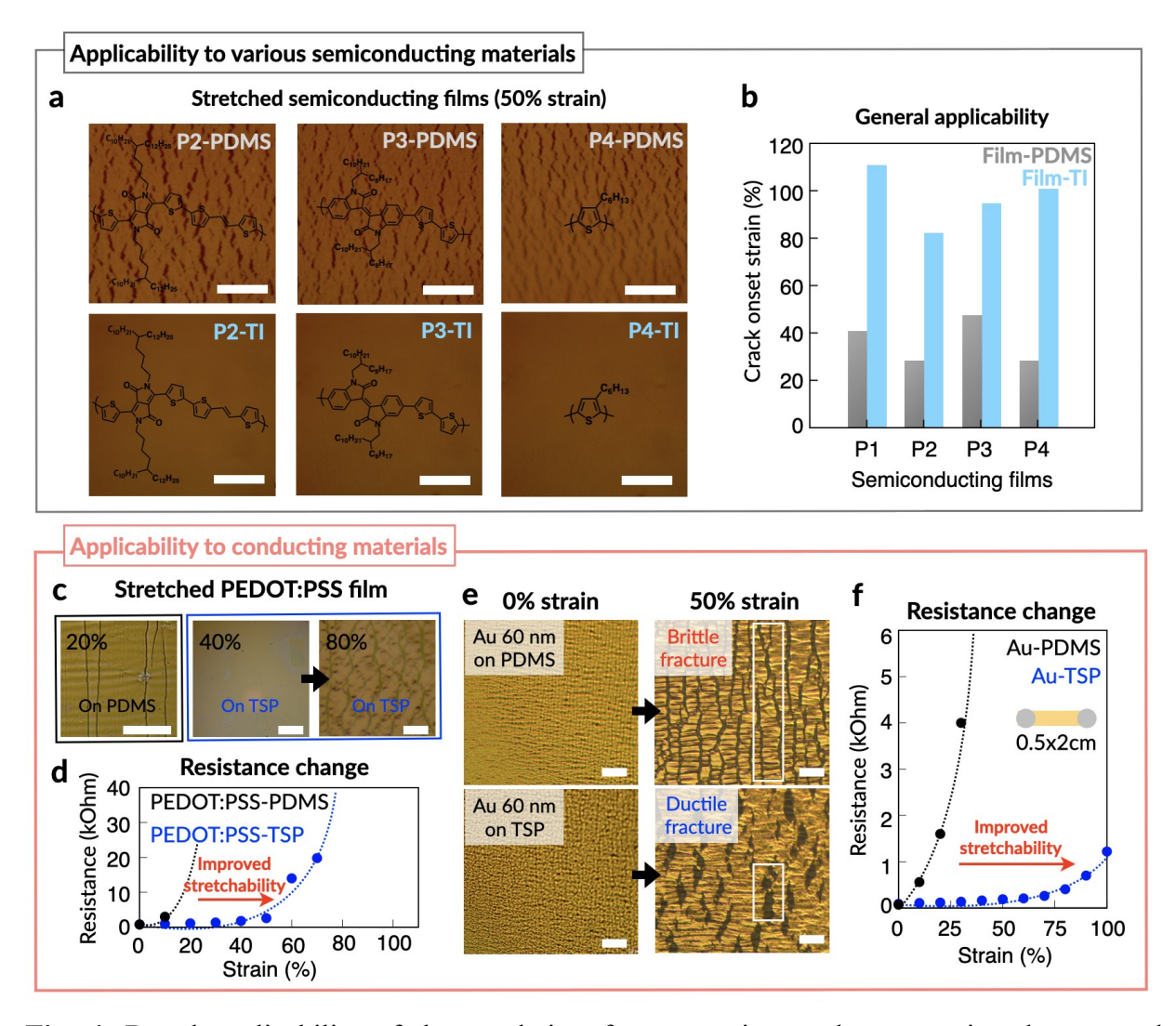


Fig. 4. Broad applicability of the tough interface to various polymer semiconductors and conductors. **a,** Optical microscope images of Px-PDMS (top) and Px-TI (bottom) (x=2, 3, 4) at 50% strain. **b,** Summary of crack onset strains of Px films (x=1, 2, 3, 4) with respect to various interface conditions. **c,** Optical microscope images of stretched PEDOT:PSS films: PEDOT:PSS on PDMS at 20% strain (left), PEDOT:PSS on TI at 40% (middle) and 80% (right) strain. PEDOT:PSS film was directly spin coated on oxygen plasma treated-PDMS and -TSP. **d,** Electrical resistance changes of PEDOT:PSS film during stretching. **e,** Optical microscope images of Au films on PDMS (top) and TSP (bottom) at 0% strain (left) and 50% strain (right), respectively. **f.** Electrical resistance changes of Au films during stretching. (Scale bar: 20 μm)